

Diffeomorphism Neural Operator for various domains and parameters of partial differential equations

Zhiwei Zhao^{†,1}, Changqing Liu^{†,1}, Yingguang Li^{*,1}, Zhibin Chen¹, Xu Liu²

¹: College of Mechanical and Electrical Engineering, Nanjing University of Aeronautics and Astronautics, Nanjing 210016, China

²: School of Mechanical and Power Engineering, Nanjing Tech University, Nanjing 211800, China

* Corresponding author.

E-mail address: liyingguang@nuaa.edu.cn (Y. Li).

[†] These authors contributed equally to this work.

Abstract:

Many science and engineering applications demand partial differential equations (PDE) evaluations that are traditionally computed with resource-intensive numerical solvers. Neural operator models provide an efficient alternative by learning the governing physical laws directly from data in a class of PDEs with different parameters, but constrained in a fixed boundary (domain). Many applications, such as design and manufacturing, would benefit from neural operators with flexible domains when studied at scale. Here we present a diffeomorphism neural operator learning framework towards developing domain-flexible models for physical systems with various and complex domains. Specifically, a neural operator trained in a shared domain mapped from various domains of fields by diffeomorphism is proposed, which transformed the problem of learning function mappings in varying domains (spaces) into the problem of learning operators on a shared diffeomorphic domain. Meanwhile, an index is provided to evaluate the generalization of diffeomorphism neural operators in different domains by the domain diffeomorphism similarity. Experiments on static scenarios (Darcy flow, mechanics) and dynamic scenarios (pipe flow, airfoil flow) demonstrate the advantages of our approach for neural operator learning under various domains, where harmonic and volume parameterization are used as the diffeomorphism for 2D and 3D domains. Our diffeomorphism neural operator approach enables strong learning capability and robust generalization across varying domains and parameters.

Keywords: Neural Operator, Diffeomorphism, Partial Differential Equations

Main

Deep learning has been successfully used to simulate computationally expensive complex physical systems described by partial differential equations (PDEs) with multiple initial and boundary conditions defined on geometry domains and achieve noteworthy performance in numerous tasks including mechanics, thermal transport, fluid dynamics and climate models, etc¹⁻⁸. A large number of applications need to obtain PDE solution on initial and boundary conditions defined in various domains, such as geometry structural optimization in design and process optimization in engineering⁹⁻¹¹. A more recent approach is to consider differential operators as maps between function spaces and learn the governing physical laws directly from

data in a class of PDEs with different parameters of initial/boundary conditions, which is named neural operator¹²⁻¹⁵. In the past years, to expand the scope of neural operators, attention has been paid to researches of complex geometry^{16,17}, symmetry characteristics¹⁸, physics fields laws¹⁹ and applications on weather prediction and heterogeneous material modeling and so on²⁰⁻²⁴. However, the existing neural operator frameworks only focus on the problem with fixed domain, which needs to be retrained after the tiny change of the domain, and the time and training cost are high. A general framework for various domains and parameters has not been thoroughly studied and remains challenging. Although there are attempts to solve the problem on various domains through transfer learning²⁵ and expanding a larger domain²⁶, there still exist a series of problems such as the requirements of a larger number of labelled data and limited generalization ability. Operators are usually maps in a particular function space, so the challenge for operators that apply to various domains is to learn a function map in a common space among a series of varying spaces.

Here, we propose a general neural operator framework, named diffeomorphism neural operator framework, which can construct an operator on various domains and parameters, where the domains are diffeomorphism (Fig. 1a). In this paper, the problem of learning function mappings in varying domains (spaces) is transformed into the problem of learning operators on a shared diffeomorphic domain. Diffeomorphism maps different domains to a shared domain, along with the parameter functions defined on them. Then, operators learn the mapping between parameter and domain function to solution function on this shared domain (Fig. 1c). The trained neural operator can be also generalized to the domains with the different shapes. The diffeomorphism operator framework is flexible in the selection of diffeomorphism algorithms and neural operator algorithms. Here, harmonic mapping algorithm and Fourier neural operator (FNO) (Fig. 1b) are adopted in 2d Darcy, pipe and airfoil fluid dynamics cases, and architecture combining volume parameterization mapping algorithm and FNO is applied to 3D mechanics problems to verify the generality, accuracy and generalization of the proposed method on varying domains with different shapes. Meanwhile, a method to evaluate the generalization ability of operators on domains is provided, in which the diffeomorphism reachability between the generalization domain and the source (training) domain is evaluated by the similarity of geometries in the shared domain.

Results

Overview of diffeomorphism neural operator framework

In a class of PDE problems, a PDE is defined on a series of bounded domains $\Omega = \{\Omega_1, \dots, \Omega_n\}$ with different shape. In each domain Ω_i , there are varying initial/boundary conditions a_i , and its solution u_i . Assume that for each domain Ω_i , there is a solution operator $\mathcal{G}_i: a_i \rightarrow u_i$. Here we want to construct an operator \mathcal{G}_1 to represent all the solution operators $\mathcal{G} = \{\mathcal{G}_1, \dots, \mathcal{G}_n\}$ in domains Ω .

The proposed framework maps all the domains Ω (physics domain) with the domain Ω_i , the associated parameter functions a_i , solution function u_i of each domain through different diffeomorphisms $\phi = \{\phi_1, \dots, \phi_n\}$ to a shared domain Ω_1 (Fig. 1(c)). Then, the mapping

relationships between the functions $a^l = \{a_1^l, \dots, a_n^l\}$ and $u^l = \{u_1^l, \dots, u_n^l\}$, where $a_i^l = \phi_i(a_i(x_i))$ and $u_i^l = \phi_i(u_i(\Omega_i))$, are learned in the shared domain Ω_1 by operator \mathcal{G}_1 .

$$\mathcal{G}_1 : (a_i^l, \Omega_i) \rightarrow u_i^l \text{ for } \Omega_i \subseteq \Omega \quad (1)$$

Because the diffeomorphism ϕ is a continuously differentiable mapping, meaning both ϕ_i and ϕ_i^{-1} are continuously differentiable. Therefore, after training the neural operator \mathcal{G}_1 , u_i could be get by $u_i = \mathcal{G}_1(a_i) = u_i^l \circ \phi_i^{-1} = \mathcal{G}_1(a_i^l, \Omega_i) \circ \phi_i^{-1}$. The schematic of the proposed approach is presented in Fig. 1. More details about the differential homeomorphism algorithm, architecture of neural operators, and the method to compute shared domains are presented in the section **Method**.

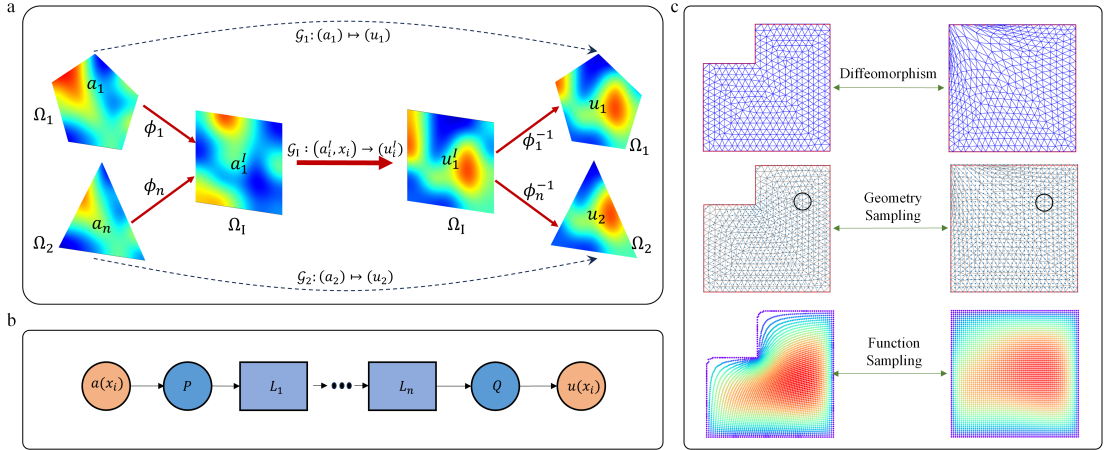


Fig. 1 | Diagram of Diffeomorphism neural operators: (a) Framework of the proposed method. (b) The neural operator used in this paper, which is Fourier Neural Operator. (c) The data processing process, which includes diffeomorphism of the physical domain to the shared domain, sampling the geometric parameters in the physical domain in terms of coordinates positions according to the sampling rule in the shared domain, and finally sampling the parameter and solution function according to the sampling positions in the physics domain.

Darcy Flow equations

Darcy's law characterizes the pressure of a fluid flowing through a porous medium with a specified permeability. A steady-state of the Darcy Flow equation is considered, which PDE is a second order, linear, elliptic PDE with a Dirichlet boundary. It has numerous applications including modeling the pressure of subsurface flow, the deformation of linearly elastic materials, and the electric potential in conductive materials. For a domain $\Omega_i \in \Omega$, the steady-state of the 2D Darcy Flow equation satisfies the following equation.

$$-\nabla \left(a(x, y) \nabla (u(x, y)) \right) = F(x, y) \quad (x, y) \in \Omega_i \quad (2)$$

$$u(x, y) = 0 \quad (x, y) \in \partial\Omega_i \quad (3)$$

where the $a(x, y)$ is the diffusion coefficient and the $F(x, y)$ is the forcing function.

Here our goal is to train a neural operator \mathcal{G}_1 , which maps the coefficient function $a(x, y)$ to the solution function $u(x, y)$ on various domains Ω . To generate the data to train the diffeomorphism neural operator, a number of domains and coefficient functions are designed. The domain Ω_i is designed as pentagon with various shape (More details see Fig. 2b and

Supplement I). The coefficient function a is defined as a random process $a = \psi(c_1, c_2, x)$, where c_1, c_2 follow a uniform distribution of 0.20 to 0.80, and the function $\psi = c_1 * \sin(x/10) - c_2 * x * (x - 10) + 2$. The architecture of diffeomorphism neural operator is a combination of harmonic mapping and Fourier Neural Operator (FNO) (Fig. 2a), and the shared domain is a square with a size of $\Omega_1 = [0,1] \times [0,1]$ and a resolution of 128×128 .

The neural operator is trained with a number of 200 generated samples using L2 loss function (**Method**) and accurately predicts the solution function on the pentagon test set with random generated pentagon shape and parameter functions. Meanwhile, the proposed model maintains the mesh invariance characterizes of the neural operator and predicts accuracy is consistent on both 256 and 512 resolutions data set (Fig. 2c). Further, the generalization of neural operators on the domains is fully verified, including the variation of size and shape. First, the neural operator is tested on the 1 to 2 magnification domains, and the prediction effect remained basically stable (Fig. 2d). Because different shapes can all be mapped to the same shared domain by diffeomorphism, we further verify the neural operator generalization trained on the pentagon data set to hexagon. The experimental results show that the diffeomorphism neural operator can maintain stable prediction accuracy even if the geometry changes greatly (Fig. 2e). We provide evaluation criteria called domain diffeomorphism similarity (DDS) for generalization of diffeomorphism neural operator on unseen domains. The relationship between DDS and generalization error on hexagon dataset is shown in Fig. 2f, which shows a strong correlation between the DDS and prediction error, indicating that the DDS can be used as a means to evaluate the generalization of diffeomorphism neural operators.

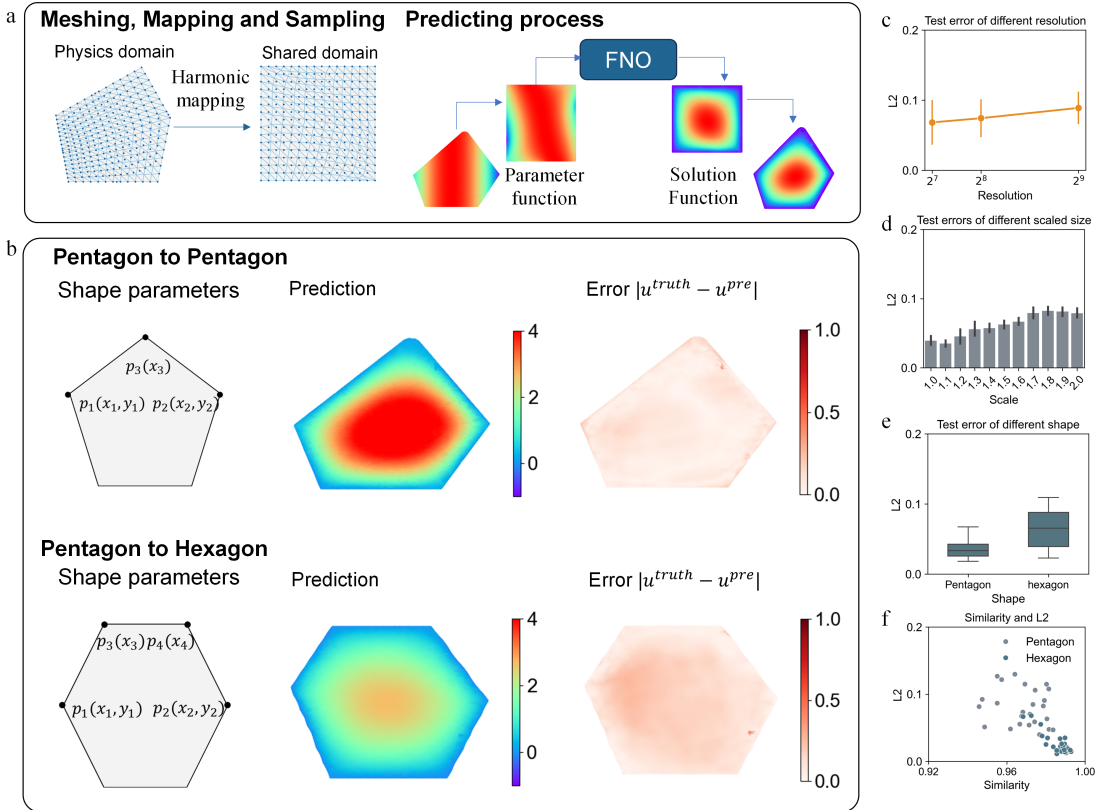


Fig. 2 | Application of diffeomorphism neural operator of Darcy flow cases on 2D domains. (a) The data process of meshing, diffeomorphic mapping and function sampling of parameter and solution

function in Darcy Flow case. (b) An indication of test cases on pentagon domain and hexagon domain. (c)-(e) Test errors in different test cases. (f) Relationship between geometric similarity on shared domain and prediction error.

Fluid Dynamics equation

Fluid dynamics plays a pivotal role in various engineering disciplines, which enables engineers and scientists to analyze and optimize designs for various systems, ranging from aircraft and automobiles to pipelines and environmental flows. Most fluids can be modeled with the incompressible Navier-Stokes (N-S) equations, which are non-linear equations that describe the interplay of a velocity field \mathbf{v} and a pressure field p within a fluid domain Ω_i :

$$\rho \left(\frac{\partial \mathbf{v}}{\partial t} + (\mathbf{v} \cdot \nabla) \mathbf{v} \right) = -\nabla p + \mu \Delta \mathbf{v} + \mathbf{f} \quad (4)$$

$$\nabla \cdot \mathbf{v} = 0 \quad (5)$$

where μ is the viscosity, ρ is the fluid density.

The traditional approach to solving fluid equations requires significant computational resources and time. Each change of geometric or parameters need rerunning simulations, posing a significant challenge for optimization problems in engineering. Here, the proposed diffeomorphism neural operator is utilized to solve this problem by rapidly generating solutions to flow fields on various domains and parameters. We have tested this approach on two typical fluid problems: pipe flows and airfoil flows.

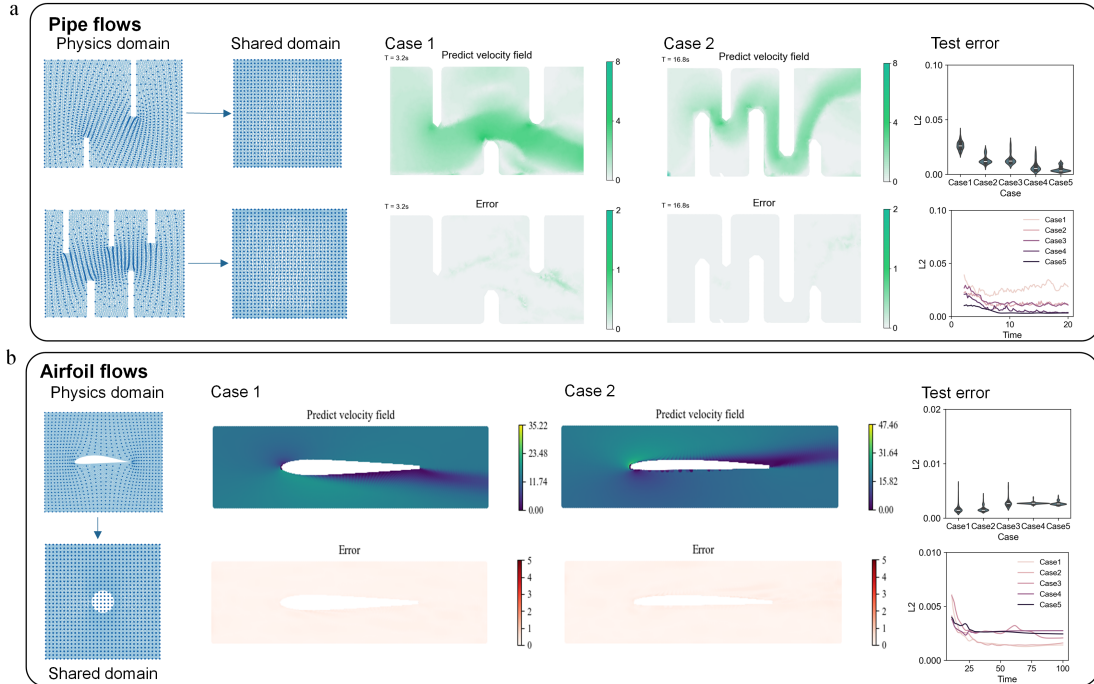


Fig. 3 | Application of diffeomorphism neural operator of flow dynamics cases on 2D domains. (a) Schematic of diffeomorphic mapping and test results of test cases in pipe flow case. (b) Schematic of diffeomorphic mapping and test results of test cases in airfoil flow case.

For pipe flows problem, the domain of the N-S equation consists of the domains with varying numbers of baffles (range from 2 to 6) and changes in baffle positions and sizes. The initial velocity in each domain follows a random process, with values randomly selected between 1

and 4. The architecture of the diffeomorphism neural operator combines harmonic mapping approach and the FNO. Initially, different pipe geometries are mapped to a shared square domain (Fig. 3a). Subsequently, the neural operator is trained on a dataset comprising 200 samples.

For airfoil flow problem, the PDE equation is described by the Reynolds-Averaged Navier-Stokes (RANS) equations, which are derived from the more fundamental Navier-Stokes (NS) equations by introducing additional terms to model turbulent effects. In this case, the varying domain comprises different airfoil shapes, while the parameters undergoing variation include the Reynolds number (range from 0.5 to 5 million) and angle of attack (ranging of ± 22.5 degrees). The airfoil shapes are obtained from the UIUC database. The architecture of diffeomorphism neural operator combines the harmonic mapping approach with the FNO. Here, the domains containing airfoil shapes are diffeomorphic mapped into a square domain with a circular shape in the center (Fig. 3b). The training dataset is generated randomly from the flow conditions described above, comprising a total of 100 samples of different airfoil shapes.

In the experiments of pipe flow and airfoils flow, our proposed framework shows its capability to predict solutions of complex fluid dynamics equations. After training on a number of domains, it accurately predicts fluid behaviors in various domains and field parameters. Moreover, it maintains stable predictions accuracy over time. This offers a viable approach to accelerate the design of pipe and airfoil shapes, where extensive testing of various parameters and shapes is required.

Mechanics equation of residual stress field and deformation

The mechanical equation of varying stress field and deformation field for various geometry domains serves as an experimental case. This is a common equation used in various engineering scenarios, such as in subtractive manufacturing, where material removal induces geometric changes, leading to different deformation fields in the initial residual stress field. Here, the machining deformation prediction of aircraft structural parts in subtractive manufacturing is taken as an example, which is a problem of solving partial differential equations with domain and parameter function changes by machining. In subtractive manufacturing, the geometric change caused by machining has a great influence on deformation, so the geometric change is as important as the change of the residual stress field for predicting deformation. The deformation field of a part is affected by the residual stress field inside the part and the geometry of the part, and its relationship is governed by the following PDE, for $\Omega_i \subseteq \Omega$,

$$\nabla \sigma(x, y, z) + \nabla (c \nabla u_{u, \Omega_i}(x, y, z)) = 0 \quad (x, y, z) \in \Omega_i \quad (6)$$

$$u_{u, \Omega_i}(x, y) = 0 \quad (x, y) \in E \quad (7)$$

where the $\sigma(x, y, z)$ is the initial residual stress, which is the parameter function in this example. $\Omega_i \in \Omega$ is the geometry of the part, which changes as the machining process. E is the boundary condition points, which represents the constraint point of the part. $u_{x, \Omega_i}(x, y, z)$ is the deformation function of the part.

Here, the aircraft structural parts with typical pocket characteristics are selected as the test example, where the domains Ω is a series geometric shapes of the aircraft structural parts generated in machining process. Because the geometric domains are 3D geometry with

complex boundaries, the architecture of diffeomorphism neural operators is a combination of a volume parameterization (Supplement III) of diffeomorphic mapping and Fourier neural operator. The shared domain is a cuboid with a size of $\Omega_1 = [0,600] \times [0,240] \times [0,30]$, which is the cover of all the geometries (Fig. 4b). The data generation process includes a random residual stress fields $\sigma(x, y, z) = c \times \sigma_0(x, y, z)$, where c ranges from 0.85 to 1.15 and the function $\sigma_0(x, y, z)$ is the initial residual stress field of the part obtained by die forging simulation. There a number of 12 domains generated in machining process of a part with 6 pockets, the data generated on the first 10 domains are used as training sets and test set, and the L2 error of the test set is 0.041. To validate the generalization, the neural operator predicts the deformation solution on the dataset of last two domains of the part, the L2 error is 0.044. In addition, the neural operator also performs deformation prediction on a part of different structure (different number and position of pockets), where the L2 error is 0.073 (Fig. 4c).

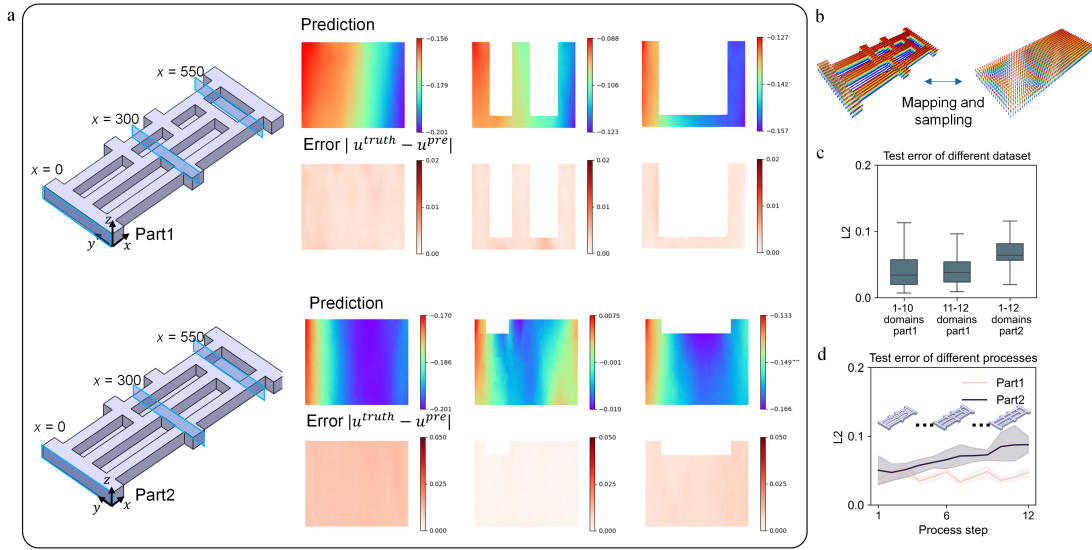


Fig. 4 | Application of diffeomorphism neural operator of deformation prediction cases on 3D domains. (a) Some test cases of prediction on part1 and part2. (b) Diffeomorphic mapping process from part domain to shared domain. (c) Test and generalization results on different dataset. (d) Test results along with the machining processes.

Methods

Diffeomorphism of different domains based on harmonic mapping

To establish the diffeomorphic mapping from any physics domain $\Omega_i \subseteq \Omega$ to shared domain Ω_1 , the harmonic mapping²⁷ is used here. Harmonic mapping is a useful tool for constructing diffeomorphisms under the conditions of conformal and bijective. It is assumed that physics domain is Ω_i with a boundary B_i , the shared domain is Ω_1 with a boundary B_1 . Firstly, the domain Ω_i is parameterized by meshing method, such as triangular mesh. Given two domains Ω_i and Ω_1 , the mapping f from Ω_i to Ω_1 is harmonic if it satisfies the equation,

$$\Delta f = 0 \quad (8)$$

where Δ is Laplacian operator on the meshed domain manifold Ω_i . Suppose that Ω_i is meshed with vertexes $\mathbf{X}^i = (\mathbf{x}_1^i, \mathbf{x}_2^i, \dots, \mathbf{x}_n^i)$, where \mathbf{x}_i^i is the coordinates vector of vertex. The purpose of a mapping f is to find the corresponding vertexes coordinates in the shared domain. For the

discrete meshing domain Ω_i , the Laplacian operator can be defined in the discrete form, and it can be computed for each vertex of the mesh using the following formula,

$$(\Delta f)_i \approx \sum_j w_{ij} (f_j - f_i) \quad (9)$$

where f_i and f_j are the value of the mapping f at the vertexes i and j , i.e., the mapped vectors in Ω_1 , and w_{ij} is the weight of the edge e_{ij} connecting the vertexes i and j in Ω_i . To calculate the weights w_{ij} , one common approach is to use the cotangent formula, which assigns a weight of 1/2 times the cotangent of the angle between adjacent triangles to each edge in the mesh, as shown in Eq.(10) and Fig. 5a.

$$w_{ij} = \frac{1}{2} * (\cotan \alpha_{ij} + \cotan \beta_{ij}) \quad (10)$$

where α_{ij} and β_{ij} are the two angles of edge e_{ij} .

This formula ensures that the weights are positive and that they sum up to the total area of the mesh. This approximation assumes that the mapping f changes linearly between neighboring vertices on the mesh, and it can be further refined by using a weighted average of the values of the function at the neighboring vertices. The Laplacian operator can then be expressed as a matrix using cotangent weights, so that the equation could be rewritten as,

$$\mathbf{L}\mathbf{f} = \mathbf{b} \quad (11)$$

$$L_{i,j} = \begin{cases} 1 & i = j \text{ and } i \in B_p \\ -w_{ij} & (i,j) \notin B_p \\ 0 & \text{otherwise} \end{cases} \quad (12)$$

where \mathbf{L} is the Laplacian matrix of the domain meshes in Ω_i , \mathbf{f} is an unknown vectors of the of the mapping function at the vertexes of the mesh in Ω_1 , i.e., $\mathbf{f} = (\mathbf{x}_1^l, \mathbf{x}_2^l, \dots, \mathbf{x}_n^l)$, and \mathbf{b} is the vector of vertexes on boundary B_l .

To map the manifold Ω_i into the same input manifold Ω_1 , the fixed boundary conditions (Dirichlet conditions) are used to solve the mapping solution, which imposes that the vectors within the domain are harmonic. Considering the boundary conditions into the \mathbf{L} and \mathbf{b} , the modified equation is $\mathbf{L}_1\mathbf{f} = \mathbf{b}_1$. After solving the linear functions, the vectors \mathbf{f} of meshes in domain Ω_1 could be obtained.

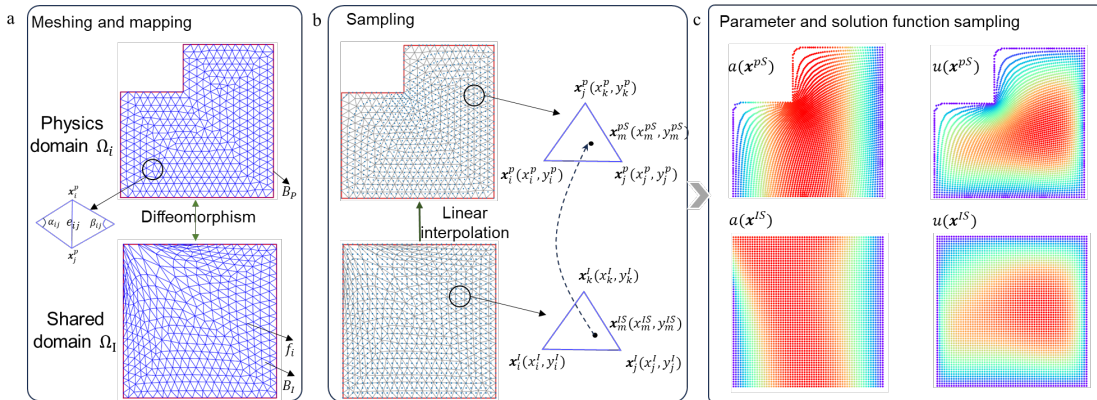


Fig. 5 | Diffeomorphism between physics and domain based on harmonic mapping. (a) Calculation flow diagram of harmonic mapping. (b) sampling method based on linear interpolation. (c) Sampling process of parameter and solution function.

The mapping from different domains to the shared domain adopts the same mapping method to ensure that the mapping attributes are consistent.

The parameter function and solution function are always represented by the values of sampled vectors. Through harmonic mapping, different physics domains are mapped to the shared domain Ω_1 with the same boundary B_1 but different and irregular meshes, i.e., the mapped vectors \mathbf{f} for each physics domain. Ω_i is different. Therefore, to ensure the regular and uniform sampling of parameter function in shared domain, the interpolation mapping method is used to get corresponding vectors and values in physics domain.

As for any new sampling point in shared domain from uniform sampling, its coordinates could be linearly interpolated by the known vectors \mathbf{f} . And for each vector \mathbf{f}_i in shared domain, there is always a corresponding vector \mathbf{v}_i with coordinates. Therefore, to get the coordinates of the corresponding point in physics domain, the interpolation weights of shared domain could be used to calculate. Take the 2D plane for example, suppose that the uniform grid point vector of the shared domain is $\mathbf{x}_m^{IS}(x_m^{IS}, y_m^{IS})$, the sampled vector of the physics domain after interpolation is $\mathbf{x}_m^{pS}(x_m^{pS}, y_m^{pS})$. The calculation process of (x_m^{pS}, y_m^{pS}) is shown in below,

$$\alpha = \frac{-(x_m^{IS} - x_j^I)(y_k^I - y_j^I) + (y_m^{IS} - y_j^I)(x_k^I - x_j^I)}{-(x_i^I - x_j^I)(y_k^I - y_j^I) + (y_i^I - y_j^I)(x_k^I - x_j^I)} \quad (13)$$

$$\beta = \frac{-(x_m^{IS} - x_k^I)(y_i^I - y_k^I) + (y_m^{IS} - y_k^I)(x_i^I - x_k^I)}{-(x_j^I - x_k^I)(y_i^I - y_k^I) + (y_j^I - y_k^I)(x_i^I - x_k^I)} \quad (14)$$

$$\gamma = 1 - \alpha - \beta \quad (15)$$

$$x_m^{pS} = \alpha \times x_i^p + \beta \times x_j^p + \gamma \times x_k^p \quad (16)$$

$$y_m^{pS} = \alpha \times y_i^p + \beta \times y_j^p + \gamma \times y_k^p \quad (17)$$

where α , β and γ are interpolation weights calculated based on linear barycentric interpolation. (x_i^I, y_i^I) , (x_j^I, y_j^I) and (x_k^I, y_k^I) are the coordinates of three points of the triangle covering sampled points \mathbf{x}_m^{IS} . (x_i^p, y_i^p) , (x_j^p, y_j^p) and (x_k^p, y_k^p) are the coordinates of the corresponding points of triangle in physics domain. After calculating all the sampling points in physics domain, the parameter function $a(\mathbf{x})$, $\mathbf{x} \in \mathbf{P}$, in physics domain Ω_i could be expressed as $a(\mathbf{x}^{pS})$. In neural operator learning process, the function $a(\mathbf{x}^{pS})$, together with \mathbf{x}^{pS} is the input of the neural network, and the $u(\mathbf{x}^{pS})$ is the output function of the neural operator. The sampling process is illustrated in Fig. 5b and Fig. 5c. It should be noted that the shared domain is the same as the output domain in this paper.

In summary, through harmonic mapping and coordinate mapping, the non-uniformly sampled data in different physics domains can be uniformly used as the input of subsequent neural operators in the shared domain.

Diffeomorphism neural operators using Fourier integral

In general, with the regular input vectors in the shared domain and the corresponding output function, neural operator could learn in the shared domain with arbitrary operator methods. FNO is chosen in this paper as the neural operator learning framework. FNO compose N-layer nonlinear operator layer K , a lifting operator P and a local projection operator Q , which is defined as follows,

$$\mathcal{G}_\theta := Q \circ \mathcal{L}_N \circ \mathcal{L}_{N-1} \circ \dots \circ \mathcal{L}_1 \circ P \quad (18)$$

where the \mathcal{G}_θ is the neural operator, the P is the lifting operator that encode the lower dimension function in the shared domain into higher dimensional space, and the Q is the projection

operator that decode the higher dimensional space into lower dimension function in the output domain. Generally, both the lifting operator P and the projection operator Q are fully neural networks. The N -layer nonlinear operator layer $\mathcal{L}_1, \dots, \mathcal{L}_N$ has the same structure as follows,

$$\mathcal{L}_N I(\mathbf{x}) = \sigma(W_N I(\mathbf{x}) + b_N I(\mathbf{x}) + (K_N(\theta)I)(\mathbf{x})) \quad (19)$$

where I is the uniform sampled input vector function, σ is non-linear activation functions, the weight matrix W_N and the bias b_N define an affine pointwise mapping $W_N I(\mathbf{x}) + b_N(\mathbf{x})$. The $(K_N(\theta)I)(\mathbf{x})$ is a non-local linear operator which could achieve the richness of linear operators in infinite dimensional setting, and it could be defined as follows,

$$(K_N(\theta)I)(\mathbf{x}) = \mathcal{F}^{-1}(P_\theta(k) \cdot \mathcal{F}(I)(k))(\mathbf{x}) \quad \forall \mathbf{x} \in \mathbb{T}^d \quad (20)$$

where the P_θ is a full matrix, \mathcal{F} and \mathcal{F}^{-1} are fast Fourier and inverse Fast Fourier transformation.

Then the component of diffeomorphism of physics domain and shared domain is combined with the FNO component, forming the diffeomorphism neural operator, which could adapt to different physics domains.

First, the mapping of different physical domains to the same shared domain is established through harmonic mapping, and then the FNO is used to learn in the differential isomorphism domain. Based on the guarantee of the general principle of invariance, FNO could learn the shared physical law in the diffeomorphic domain and realize the invariance of the domain.

The diffeomorphism neural operator establishes a mapping relationship between regular sampling of input function to output function in the shared domain. Then the neural operator \mathcal{G}_θ could be defined as to achieve the map between input function to output function, i.e., $\mathcal{G}_\theta: (a(\mathbf{x}^{pS}), \mathbf{x}^{pS}) \rightarrow (u(\mathbf{x}^{pS}))$, where \mathcal{G}_θ is parametrized by θ . The learning objective can be defined as to minimizing the empirical loss on dataset $\{a(\mathbf{x}^{pS}), \mathbf{x}^{pS}, u(\mathbf{x}^{pS})\}$. The loss function is based on L2 Relative error, as shown in below,

$$\begin{aligned} Loss &= E_{\Omega_i \sim \Omega, \mathbf{x}^{pS} \sim \Omega_i, a \sim \sigma, d \sim \omega} \frac{\|\mathcal{G} - \mathcal{G}_\theta\|^2}{\|\mathcal{G}\|^2} \\ &= \frac{1}{N * M} \sum_{i=1}^N \sum_{j=1}^M \frac{\|u_i^{truth}(\mathbf{x}_{ij}^{pS}) - u_i^{pre}(\mathbf{x}_{ij}^{pS})\|^2}{\|u_i^t(\mathbf{x}_{ij}^{pS})\|^2} \end{aligned} \quad (21)$$

where u_i^{truth} and u_i^{pre} are predicted and truth solution function sampled by \mathbf{x}_{ij}^{pS} (total M sampled points) in the i^{th} domain (total N domains).

Generalization evaluation of diffeomorphism neural operators through geometric similarity on shared domain

One of the primary goals of most machine learning algorithms is to generalize to unseen data. For diffeomorphism neural operators, there have been some validations of generalizing to unseen domains. However, ensuring and quantifying generalization remains an open and challenging problem. For machine learning, the evaluation of generalization ability concerns the similarity between data. Here, we focus on the generalization of neural operators across different domains. The diffeomorphism neural operator learns mappings between parameter equations and solution equations in a shared domain. According to the sampling process

mentioned above, both parameter functions $a(\mathbf{x}^{pS})$ and solution functions $u(\mathbf{x}^{pS})$ can be seemed as mappings on geometric parameters \mathbf{x}^{pS} in the original domain. Therefore, the generalization ability of the diffeomorphism neural operator is mainly influenced by geometry domains. Consequently, evaluating the similarity between different domains is a direct approach to assess the generalization of neural operator. Here, we introduce an approach called domain diffeomorphism similarity (DDS) to evaluate the generalization of diffeomorphism neural operators on unseen domains. Specifically, the DDS evaluates the similarity between geometries mapped from two different domains in a shared domain.

Consider ϕ_i and ϕ_j two diffeomorphisms from domain Ω_i and Ω_j to shared domain Ω_1 , the domain parametrization function is \mathbf{x}_i^{pS} and \mathbf{x}_j^{pS} . Our goal is to evaluate the similarities between \mathbf{x}_i^{pS} and \mathbf{x}_j^{pS} . Actually, \mathbf{x}_i^{pS} and \mathbf{x}_j^{pS} could be regarded as two geometric images²⁷ in the shared domain space. Therefore, we utilize the Normalized Cross-Correlation (NCC) to evaluate the similarity between the two geometric images with size of $M \times N \times C$ (For a 2D domain with a resolution of 128, the size is $128 \times 128 \times 2$), which could be expressed as,

$$NCC(\mathbf{x}_i^{pS}, \mathbf{x}_j^{pS}) = \frac{\sum_{l=1}^{MN} \sum_{c=1}^C (x_{i,n,c}^{pS} - \overline{x_{i,c}^{pS}})(x_{j,n,c}^{pS} - \overline{x_{j,c}^{pS}})}{\sqrt{\sum_{l=1}^{MN} \sum_{c=1}^C (x_{i,n,c}^{pS} - \overline{x_{i,c}^{pS}})^2} \sqrt{\sum_{l=1}^{MN} \sum_{c=1}^C (x_{j,n,c}^{pS} - \overline{x_{j,c}^{pS}})^2}} \quad (22)$$

where $\overline{x_{i,c}^{pS}}$ and $\overline{x_{j,c}^{pS}}$ is the average values of tensor $\mathbf{x}_i^{pS}, \mathbf{x}_j^{pS}$ on dimension c . This formula describes the similarity between two domains with multiple dimensions. In order to evaluate whether the trained operator can generalize to other domains, the NCC between the domain that needs to be generalized and the domain in the training set is calculated and the average value is taken as the index, i.e., DDS, to evaluate the generalization of this domain. The results of DDS and generalization error are shown in the Fig. 2f, and there is a strong correlation between the DDS and prediction error, indicating that the DDS can be used as a means to evaluate the generalization of diffeomorphism neural operators.

Discussion and Conclusion

In this work, we present a general neural operator learning method to learn operators in various domains and initial/boundary conditions of PDE equations. The proposed method, i.e., diffeomorphism neural operator, learn the physics lay governed by PDE equations in a shared domain which is diffeomorphism with physics domains. The operator learning capability of the proposed method has been validated through experiments on static and dynamics PDE equations, including Darcy flow equation, N-S equations and RANS equations. Additionally, the generalization capability of the proposed framework in the domain has also been validated, including variations in size and shape. Through systematic experiments, it is evident that the method exhibits stronger operator learning capabilities, particularly in complex-various domains.

The Diffeomorphism neural operator is the first framework of operators for a PDE equation with various domains and initial/boundary conditions. The proposed framework has a wide

range of applications in science and engineering, such as optimization in product design and manufacturing process.

The proposed methods also have some limitations. For instance, the need for improvement in the operator generalization capability between two dissimilar domains. A potential direction for optimization this problem is to enhance the learning capability of operators by introducing methods based on spatial invariance, rotational invariance, and other neural network techniques.

Acknowledgements

This work was supported by the National Science Fund of China for Distinguished Young Scholars under Grant 51925505 (Yingguang Li) and National Natural Science Foundation of China under Grant 52175467 (Changqing Liu).

Competing interests

We hereby declare that prior to the formal publication of this study, we filed a patent application (No. 2023116721216) regarding the core framework of this research on December 7th, 202328, which is set to be made public on April.

Reference

1. Wang, J., Mo, Y. L., Izzuddin, B. & Kim, C.-W. Exact Dirichlet boundary Physics-informed Neural Network EPINN for solid mechanics. *Comput. Methods Appl. Mech. Eng.* **414**, 116184 (2023).
2. Pestourie, R., Mroueh, Y., Rackauckas, C., Das, P. & Johnson, S. G. Physics-enhanced deep surrogates for partial differential equations. *Nat. Mach. Intell.* **5**, 1458–1465 (2023).
3. Cai, S., Mao, Z., Wang, Z., Yin, M. & Karniadakis, G. E. Physics-informed neural networks (PINNs) for fluid mechanics: a review. *Acta Mech. Sin.* **37**, 1727–1738 (2021).
4. Yao, Y., Guo, J. & Gu, T. A deep learning method for multi-material diffusion problems based on physics-informed neural networks. *Comput. Methods Appl. Mech. Eng.* **417**, 116395 (2023).
5. Raissi, M., Perdikaris, P. & Karniadakis, G. E. Physics-informed neural networks: A deep learning framework for solving forward and inverse problems involving nonlinear partial differential equations. *J. Comput. Phys.* **378**, 686–707 (2019).
6. Gao, H., Sun, L. & Wang, J.-X. PhyGeoNet: Physics-informed geometry-adaptive convolutional neural networks for solving parameterized steady-state PDEs on irregular domain. *J. Comput. Phys.* **428**, 110079 (2021).
7. Sukumar, N. & Srivastava, A. Exact imposition of boundary conditions with distance functions in physics-informed deep neural networks. *Comput. Methods Appl. Mech. Eng.* **389**, 114333 (2022).
8. Li, Z. et al. Physics-informed neural operator for learning partial differential equations. *ArXiv Prepr. ArXiv211103794* (2021).
9. Wang, H., Planas, R., Chandramowlishwaran, A. & Bostanabad, R. Mosaic flows: A transferable deep learning framework for solving PDEs on unseen domains. *Comput. Methods Appl. Mech. Eng.* **389**, 114424 (2022).
10. Zhao, Z. et al. A subsequent-machining-deformation prediction method based on the latent field estimation using deformation force. *J. Manuf. Syst.* **63**, 224–237 (2022).
11. Shukla, K. et al. Deep neural operators can serve as accurate surrogates for shape optimization: A case study for airfoils. Preprint at <http://arxiv.org/abs/2302.00807> (2023).

12. Li, Z. et al. Fourier Neural Operator for Parametric Partial Differential Equations. Preprint at <http://arxiv.org/abs/2010.08895> (2021).
13. Kovachki, N. et al. Neural Operator: Learning Maps Between Function Spaces. Preprint at <http://arxiv.org/abs/2108.08481> (2023).
14. Li, Z. et al. Neural operator: Graph kernel network for partial differential equations. ArXiv Prepr. ArXiv200303485 (2020).
15. Lu, L., Jin, P., Pang, G., Zhang, Z. & Karniadakis, G. E. Learning nonlinear operators via DeepONet based on the universal approximation theorem of operators. *Nat. Mach. Intell.* **3**, 218–229 (2021).
16. Li, Z., Huang, D. Z., Liu, B. & Anandkumar, A. Fourier Neural Operator with Learned Deformations for PDEs on General Geometries. Preprint at <http://arxiv.org/abs/2207.05209> (2022).
17. Chen, G. et al. Learning Neural Operators on Riemannian Manifolds. Preprint at <https://doi.org/10.48550/arXiv.2302.08166> (2023).
18. Helwig, J. et al. Group Equivariant Fourier Neural Operators for Partial Differential Equations. Preprint at <http://arxiv.org/abs/2306.05697> (2023).
19. Yin, M., Zhang, E., Yu, Y. & Karniadakis, G. E. Interfacing finite elements with deep neural operators for fast multiscale modeling of mechanics problems. *Spec. Issue Honor Lifetime Achiev. J Tinsley Oden* **402**, 115027 (2022).
20. Pathak, J. et al. FourCastNet: A Global Data-driven High-resolution Weather Model using Adaptive Fourier Neural Operators. Preprint at <http://arxiv.org/abs/2202.11214> (2022).
21. Cai, S., Wang, Z., Lu, L., Zaki, T. A. & Karniadakis, G. E. DeepM&Mnet: Inferring the electroconvection multiphysics fields based on operator approximation by neural networks. *J. Comput. Phys.* **436**, 110296 (2021).
22. Goswami, S., Yin, M., Yu, Y. & Karniadakis, G. E. A physics-informed variational DeepONet for predicting crack path in quasi-brittle materials. *Comput. Methods Appl. Mech. Eng.* **391**, 114587 (2022).
23. Li, W., Bazant, M. Z. & Zhu, J. Phase-Field DeepONet: Physics-informed deep operator neural network for fast simulations of pattern formation governed by gradient flows of free-energy functionals. *Comput. Methods Appl. Mech. Eng.* **416**, 116299 (2023).
24. You, H., Zhang, Q., Ross, C. J., Lee, C.-H. & Yu, Y. Learning deep Implicit Fourier Neural Operators (IFNOs) with applications to heterogeneous material modeling. *Comput. Methods Appl. Mech. Eng.* **398**, 115296 (2022).
25. Goswami, S., Kontolati, K., Shields, M. D. & Karniadakis, G. E. Deep transfer operator learning for partial differential equations under conditional shift. *Nat. Mach. Intell.* **4**, 1155–1164 (2022).
26. Lu, L. et al. A comprehensive and fair comparison of two neural operators (with practical extensions) based on FAIR data. *Comput. Methods Appl. Mech. Eng.* **393**, 114778 (2022).
27. Gu, X., Gortler, S. J. & Hoppe, H. Geometry images. in *Proceedings of the 29th annual conference on Computer graphics and interactive techniques* 355–361 (Association for Computing Machinery, New York, NY, USA, 2002). doi:10.1145/566570.566589.
28. Li, Y. et al. A method of physical field operators based on diffeomorphism and its application [P], China Patent, 2023116721216 (Dec 7th 2023).

Appendix

I. Dataset details

Table I.1 An overview of the various domains datasets.

Datasets	Train	Domain parameters	Parameter function
----------	-------	-------------------	--------------------

Darcy flow Pentagon	200	$x_1 \in [0.00, 2.00], y_1 \in [4.00, 6.00]$ $x_2 \in [8.00, 10.00], y_2 \in [4.00, 6.00]$ $x_3 \in [3.00, 7.00]$	$c_1, c_2 \in [2.00, 9.00]$
Darcy flow Hexagon	200	$x_1 \in [0.00, 2.00], y_1 \in [4.00, 6.00]$ $x_2 \in [8.00, 10.00], y_2 \in [4.00, 6.00]$ $x_3 \in [2.00, 4.00]$ $x_4 \in [6.00, 8.00]$	$c_1, c_2 \in [2.00, 9.00]$
Pipe flow	200	The number of baffles $\in [2, 6]$ Width of baffle $\in [3, 6]$ Length of baffle $\in [4, 24]$	Velocity $\in [1.0, 4.0]$
Airfoil flow	100	From UIUC database	Re $\in [0.5, 5.0]$ Attack angle $\in [-22.5, 22.5]$
Deformation	600	Depth of pocket $\in [2, 24]$ Part1 pocket number: 6 Part2 pocket number: 5	$c \in [0.85, 1.15]$

II. Neural network parameters and training parameters

Table II.1 Details of neural networks of neural operators

Experiments	Training parameters				
	Number of layers	Batch size	Learning rate	Nodes size or sample size	Epochs
Darcy flow	Fourier layer = 6 FCN layer = 4	32	0.001	128×128	800
Pipe flow	Fourier layer = 6 FCN layer = 4	32	0.001	128×128	800
Airfoil flow	Fourier layer = 6 FCN layer = 4	16	0.001	128×128	800
Deformation	Fourier layer = 6 FCN layer = 4	20	0.0001	121×19×7	800

III. Diffeomorphism base on volume parameterization

Volume parameterization

Volume parameterization is one of the common methods in the field of isogeometric analysis, which is of great significance in the fields of medical treatment and computer graphics. The goal of volume parameterization is to construct a bijective mapping between a three-dimensional manifold and a three-dimensional field with a simple regular shape. The mapping can be used to generate a canonical coordinate system on a three-dimensional manifold to simplify complex geometric processing and computer graphics problems.

The article utilizes volume parameterization to establish the diffeomorphism from the geometric domain of a 3D part to a cuboid domain. The mapping process mainly includes the following steps: (1) geometric analysis of the part, (2) determination of the shared domain, and (3) volume parameterization. Finally, we provide a proof of the diffeomorphism of volume parameterization.

(1) Geometric analysis of the structural part. The structural part selected in this paper has pocket features, which have the following characteristics: the geometric variations of the part only occur on the top surface of the part, and the cross-sections of the part along the length

direction have a genus of 0.

(2) Determination of the shared domain. According to the geometric characteristics of the part, a cuboid domain is selected as the shared domain. In order to minimize the shape distortion of the part after mapping, a cuboid domain of 600mm × 240mm × 30mm is chosen as the shared domain.

(3) Volume parameterization. The top surface, bottom surface, and two side surfaces of the die-forged structural component are expressed through functions $T(x, y)$, $B(x, y)$, $L(x, z)$, and $R(x, z)$, respectively. Then volume parameterization can be expressed by the following formula,

$$\begin{bmatrix} u \\ v \\ w \end{bmatrix} = X \left(\begin{bmatrix} x \\ y \\ z \end{bmatrix} \right) = \begin{bmatrix} \frac{240 \times (y - R(x))}{L(x) - R(x)} \\ \frac{30 \times (z - B(x, y))}{T(x, y) - B(x, y)} \end{bmatrix}; \begin{bmatrix} u \\ v \\ w \end{bmatrix} \in S_{uvw}, \begin{bmatrix} x \\ y \\ z \end{bmatrix} \in S_{xyz} \quad (\text{III-1})$$

where X represents the volume parameterization function, which is the mapping from the geometric domain of the part to the shared domain, $[u, v, w]^T$ denotes the coordinates of a point in the shared domain after mapping, and $[x, y, z]^T$ represents the coordinates of a point in the geometric domain of the part before mapping. The method can achieve mappings from domains of the similar part to the shared domain.

Proof of the diffeomorphism of volume parameterization

If the mapping X is diffeomorphism, it must be a bijection, and both the mapping X and its inverse mapping X^{-1} must be smooth mappings. From the equation of the mapping X provided and its physical meaning, it can be easily proved that the mapping in this article is bijection. Then, by demonstrating the non-zero Jacobian determinant of the mapping X , it can be proved that both the mapping X and its inverse mapping X^{-1} are smooth mappings. According to Eq.III-1, the Jacobian matrix of the mapping X is:

$$\begin{aligned} DX \left(\begin{bmatrix} x \\ y \\ z \end{bmatrix} \right) &= \begin{bmatrix} \frac{\partial X}{\partial x} & \frac{\partial X}{\partial y} & \frac{\partial X}{\partial z} \end{bmatrix} \\ &= \begin{bmatrix} 1 & 0 & 0 \\ \frac{\partial \left(\frac{240 \times (y - R(x))}{L(x) - R(x)} \right)}{\partial x} & \frac{240}{L(x) - R(x)} & 0 \\ \frac{\partial \left(\frac{30 \times (z - B(x, y))}{T(x, y) - B(x, y)} \right)}{\partial x} & \frac{\partial \left(\frac{30 \times (z - B(x, y))}{T(x, y) - B(x, y)} \right)}{\partial y} & \frac{30}{T(x, y) - B(x, y)} \end{bmatrix} \quad (\text{III-2}) \end{aligned}$$

Then, the Jacobian determinant of the mapping X is given by,

$$\det DX \left(\begin{bmatrix} x \\ y \\ z \end{bmatrix} \right) = \left(\frac{260}{L(x) - R(x)} \right) \times \left(\frac{30}{T(x, y) - B(x, y)} \right) > 0 \quad (\text{III-3})$$

Because that $L(x) - R(x) > 0$ and $T(x, y) - B(x, y) > 0$, the Jacobian determinant of the map X is always greater than 0. Therefore, both the mapping X and its inverse mapping X^{-1} are smooth maps. Therefore, the mapping X is a diffeomorphism.